Evaluation of Cloud Properties Derived from Dual-View Satellite Data over the Continental United States

J. Kirk Ayers and R. Palikonda
Analytical Services and Materials Inc.
Hampton, Virginia

P. Minnis
National Aeronautics and Space Administration-Langley Research Center
Hampton, Virginia

P. Heck
CIMSS/University of Wisconsin
Madison, Wisconsin

R. Arduini
Science Applications International Corporation
Hampton, Virginia

Corresponding Author J. Kirk Ayer (j.k.ayers@larc.nasa.gov)

Introduction

Development of a consistent, accurate quantification of the cloud field over the Atmospheric Radiation Measurement (ARM) Climate Research Facility (ACRF) Southern Great Plains site (an area with extensive surface observations) is crucial to the development of improved parameterizations in models and to providing a linkage between local and GCM grid scale observations. Satellite observations are the only practical means to acquire the necessary parameters over large domains for model evaluation, and future assimilation. Nearly continuous coverage over the United States (US) is provided by the geostationary satellites, Goddard Earth Observing System (GOES)-East (75°W) and GOES-West (135°W). These geosynchronous orbiting satellites provide the capability for performing coincident retrievals of cloud properties from different pairs of viewing angles. The amount of variation in a given retrieved property with viewing angles is a measure of the accuracy of the retrieval because, ideally, the variation should be zero. Thus, pairs of measurements form two different angles can provide an assessment of cloud retrieval algorithm performance.

Retrievals of cloud properties rely on idealized parameterizations of cloud reflectance based on assumed optical properties such as the scattering phase function. Actual cloud reflectance is influenced by three-dimensional (3D) cloud structure and variances in the phase functions that are not captured in the simple retrieval models. By viewing the same clouds simultaneously from different angles, it is possible to

estimate the uncertainties caused by the combination of the 3D effects and the model assumption. By altering model characteristics, it is also possible to study the sensitivity of the retrieval errors to the assumed model, and eventually minimize errors due to the assumed models. This paper begins that process for the ARM satellite-derived cloud properties by determining the relative errors in retrieved values of ice and liquid water cloud properties using recently available multi-satellite retrievals over common areas of the United States.

Methodology

This study uses the Visible Infrared Solar-infrared Split-window Technique (VISST) to determine cloud properties. VISST is a 4-channel model-matching method for plane parallel clouds, (Minnis et al. 2001). It uses parameterizations of radiative transfer calculations for seven water and nine ice crystal size distributions (Minnis et al. 1998) to estimate theoretical radiances that are matched with 4-km GOES-10 (G-10) and GOES-12 (G-12) 0.65, 3.9, and 10.8 μm radiances to estimate several cloud properties. Additionally, the 12.0-μm channel, missing on the G-12, is used in the analysis of the G-10 images. Atmospheric profiles of temperature and humidity derived from 40-km Rapid Update Cycle (RUC-2) hourly analyses are used to estimate the skin temperature, calculate cloud height from the derived cloud temperature, and account for atmospheric absorption in each channel. Surface type is based on the IGBP 10-minute resolution surface map. Clear-sky reflectances and ice and snow masks developed for the Clouds and the Earth's Radiant Energy System (CERES) program are used for additional surface characterization (Trepte et al. 1999). The primary products produced by VISST are pixel-level retrievals of micro and macro physical cloud properties including cloud phase, optical depth (τ), effective droplet radius (Re) or effective ice particle diameter (De), liquid water path (LWP) or ice water path (IWP), and cloud height and temperature, (Minnis et al. 2004). A secondary product of VISST is a grid-level average of the pixel-level data. The grid resolution can be specified by the user and was set to 0.5° equal angle for this study.

This study uses coincident G-10 and G-12 data from April, July, and October 2004 and from January 2005. These months were selected to account for seasonal variation in cloud properties and sun angle. The data from each month were individually screened to select three days per month to provide a near equal mix of ice and water clouds. The area selected for analysis, shown in Figure 1, is bounded by 50°N, 90°W and 25°N, 105°W. This area provides optimal satellite observation overlap and contains the ACRF SGP site, an excellent source of validation data.

Data from the satellite overlap region were analyzed with the VISST and the results were averaged into gridded network Common Data Format (NetCDF) files, similar to those used for storage in the ARM Data Archive. The G-10 and G-12 results were spatially and temporally matched and filtered to categorize clouds as primarily (>90%) ice or water phase. Only grid boxes having 100% cloud cover with a primary (>90%) phase were included in this study. After filtering for $\tau < 32$, regression analyses of various properties was performed and evaluated for agreement. Finally, an attempt to identify factors contributing to poor agreement was made.

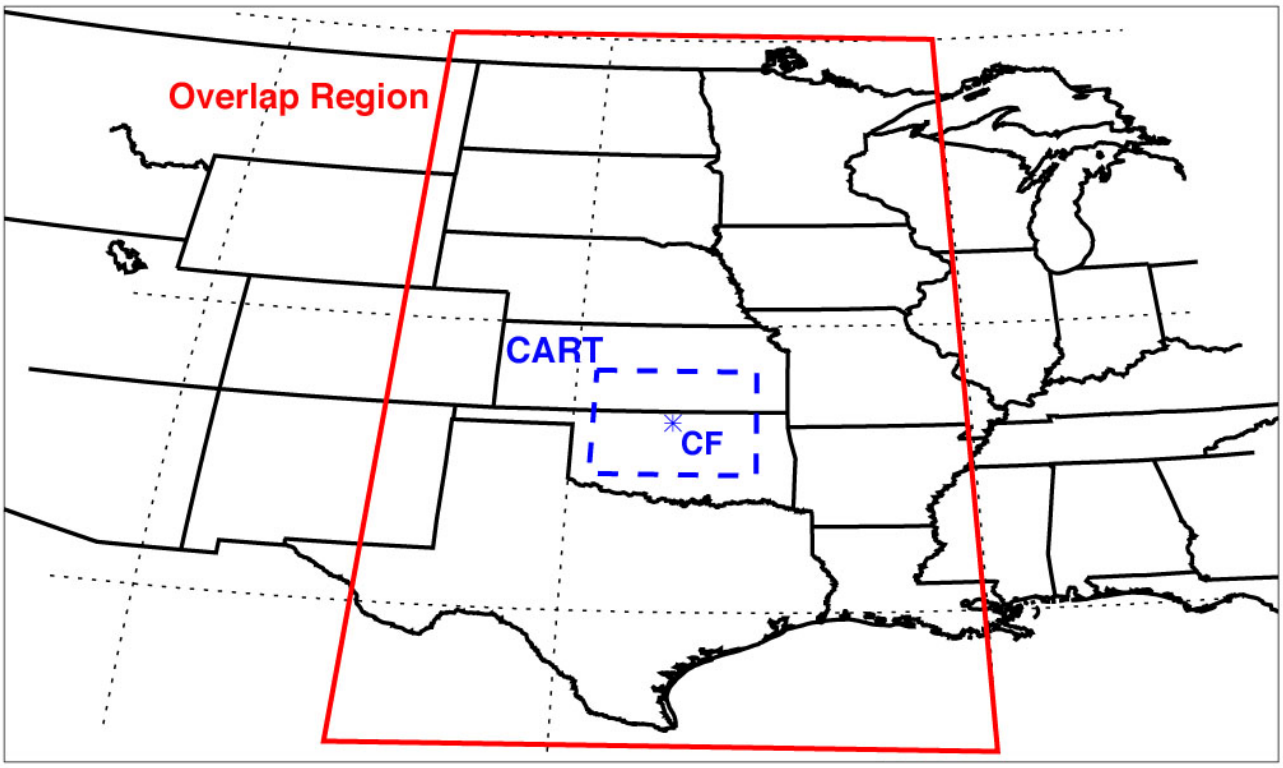

Figure 1. Overview of the satellite observation overlap analysis region.

Results

Matched grid box averages of τ and Re taken at 1845 Universal Time Coordinates (UTC) are shown in Figures 2a and b, respectively. As shown in Figure 2a, the agreement at 1845 UTC is very good with a correlation coefficient of 0.92 and a bias of -1.06. The differences seen at larger optical depths are primarily related to effects of scattering angle and idealized models. As shown in Figure 2b, the agreement between the VISST-derived values of Re is also relatively good. Generally, Re retrieved from G-10 is greater than that from G-12 for January and October, but the reverse is true for April and July. The combination of the monthly data nearly cancels the monthly biases leading to a total bias of only 0.45 μm, or 5%. The hour, 1845 UTC, was selected here because it is the image time nearest to local solar noon for the region of analysis. At local solar noon both satellites view the center of the region at nearly identical scattering angles providing the optimum comparison conditions. To determine the effect of scattering angle differences on the retrievals, similar comparisons were performed using data taken from 1415 to 2245 UTC. A summary of monthly mean τ and Re for water cloud retrievals and their associated biases and root mean square (RMS) errors are shown in Figure 3. As shown in Figure 3a, the G-10 VISST derived mean τ ranges from 10 to 20, with an associated monthly maximum bias of -3.5 (-19%) relative to τ from G-12 (Figure 3b). The monthly RMS errors (Figure 3c) range from ~1.5 to ~5 (28%). The minimum bias and RMS errors occur near 1845 UTC, as expected. Except for April, the G-10 optical depth tends to be larger during the afternoon than in the morning. Similarly, the bias is more negative in the morning. The overall mean optical depth for G-10 was 15.7 with a mean

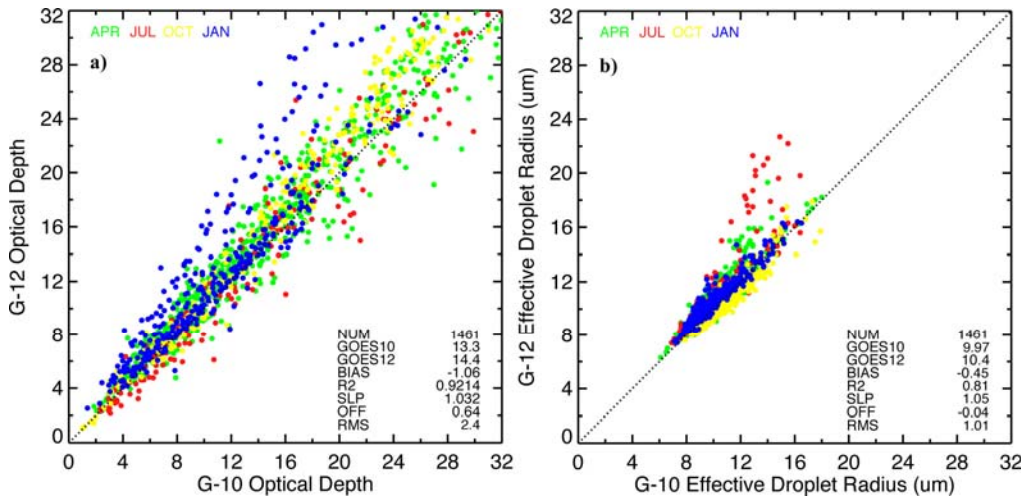

Figure 2. Comparison of VISST derived water cloud (a) optical depth and (b) effective droplet radius derived from GOES-10 and GOES-12 satellite images at 1845 UTC.

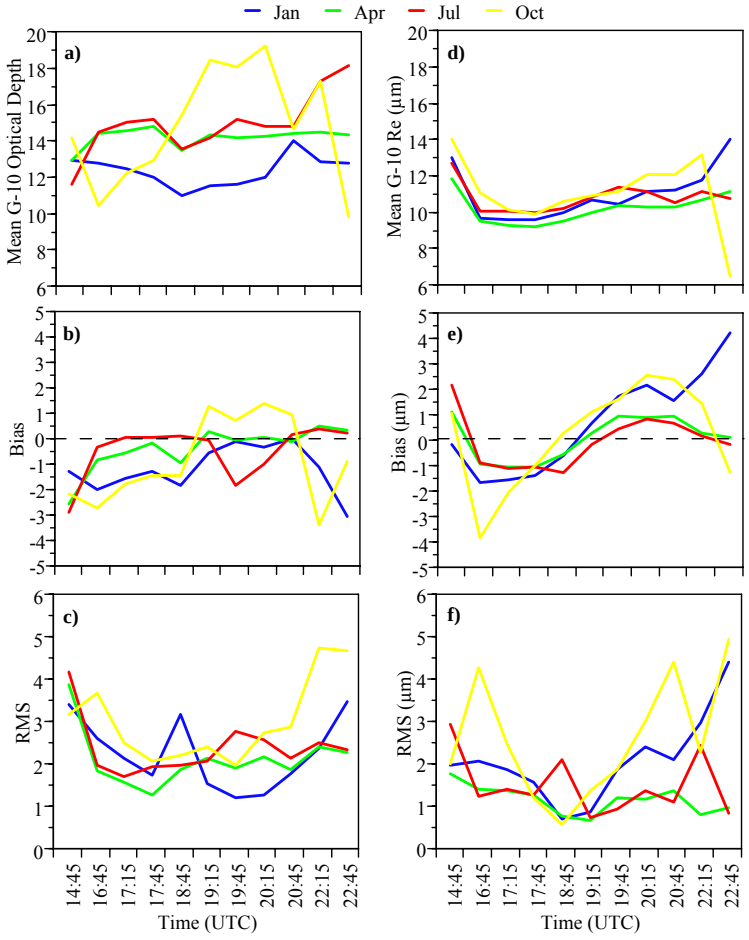

Figure 3. Summary of VISST derived G10 hourly water cloud mean τ and Re with associated biases and RMS errors from comparison to G12 retrievals for the 4 months studied.

bias of 0.86 and an RMS error of 1.4 (10%). Figure 3d shows that the monthly Re means range from 7 to 14 μm, with a monthly maximum bias (Figure 3e) of ~4.5 μm at 2245 UTC during January when the sun is in near-terminator conditions. Otherwise, except at 1645 UTC during October, the biases are typically less than 2.5 μm. Both the mean G-10 effective radii and the biases increase from morning to afternoon. The monthly RMS errors (Figure 3f) range from 0.5 to ~5.0 μm. The overall mean Re from G-10 data was 10.8 μm with a mean bias of 0.28 μm and an RMS error of 1.55 μm (15%). Effective water cloud heights and LWP were also compared. The G-10 mean cloud height of 1.99 km differed from its G-12 counterpart by only 0.01 km. On a monthly hourly basis, water cloud height RMS differences are typically < 10% but can be as large as 27% (corresponding to a 0.08 km difference). Mean biases were typically less than 0.04 km. On average, the RMS difference between the matched pairs was 0.05 km (2.5%). The LWP analysis yielded a mean of 119.8 gm^{-2} for G-10 with a mean bias of 2.6 gm^{-2} relative to G-12. The mean RMS difference for the entire dataset is 19.5 gm^{-2} (16%).

The ice cloud τ and De values retrieved at 1845 UTC for the 4 months are compared in Figures 4a and b, respectively. The overall agreement in τ (Figure 4a) at 1845 UTC is fair with a bias of 1.5 (13%) and an RMS difference of 3.9, a value of nearly 37% relative to the mean. The G10 De mean (Figure 4b) agrees very well with the G-12 values. The overall De bias is only -0.18 μm and the RMS difference is

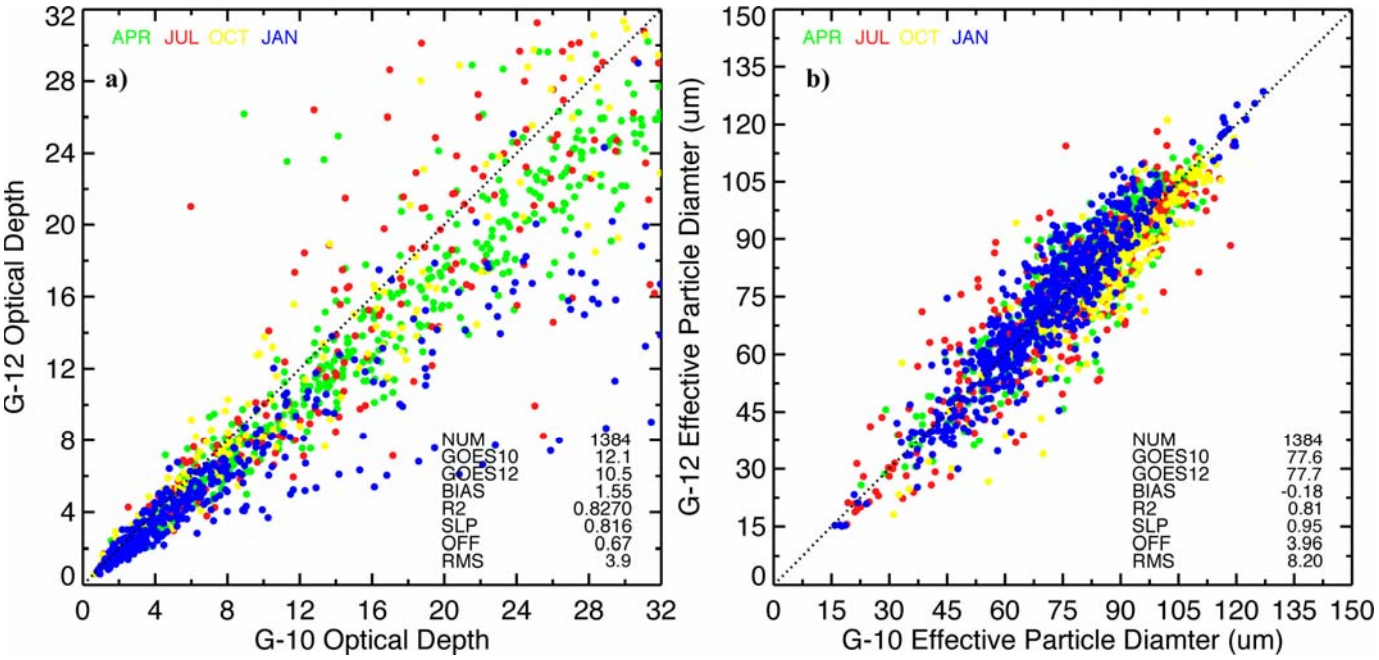

Figure 4. Comparison of VISST derived (a) ice cloud optical depth and (b) effective particle diameter derived from G-10 and G-12 satellite images at 1845 UTC.

8.2 µm (~11%). These differences vary considerably with time of day as demonstrated in Figure 5, which is the same as Figure 3 except that only ice clouds are considered. As shown in Figure 5a, the mean G-10 ice cloud τ ranges from 4 to 16, with associated monthly biases (Figure 5b) ranging from -4 to 4 relative to G-12. The monthly ice cloud RMS differences in τ range from ~3 to ~6 (Figure 5c). Even though the bias is larger than that derived from water clouds, the minimum occurs at 1845 UTC, as expected. The overall mean τ for G-10 was 12.0 with a mean bias of 0.2 and an RMS difference (Figure 5c) of 2.2 (19%) relative to the G-12 values. Like, the water clouds, the ice cloud optical depths tend to be larger during the morning than in the afternoon increasing again during late afternoon. The biases follow a similar cycle. Figure 5d afternoon increasing again during late afternoon. The biases follow a similar cycle. Figure 5d shows that the monthly mean De from G-10 ranges from 30 to 90 µm. Except for the near-terminator times in January and October, though, the range is only between 70 and 87 µm. The mean hourly differences between De from G-10 and G-12 (Figure 5e) are quite small at the near-terminator hours and as large as -23 µm at 1645 UTC during October. The monthly RMS differences in De (Figure 5f) range from 7.5 to 30 µm with the greatest values found at the near-terminator hours and at 1645 and 2045 UTC during October. The overall mean De for G-10 was 68.5 µm with a mean bias of -3.5 µm and an RMS error of 7.5 µm (10%). The G-10-derived mean ice cloud height (not shown) of 7.58 km was 0.37 km lower, on average, than the G-10 values with an RMS difference of 0.44 km (5.6%). Ice cloud height instantaneous RMS differences are typically less than 10% except during January when at some hours they increase to as much as 40%, presumably due to the occurrence of thin clouds over snow fields or over lower clouds. Mean biases are generally less than 0.5 km. The IWP analysis yielded a mean of 321 gm^{-2} from G10 with a mean bias of -3.2 gm^{-2} and mean RMS difference of 64.8 gm^{-2} (20%).

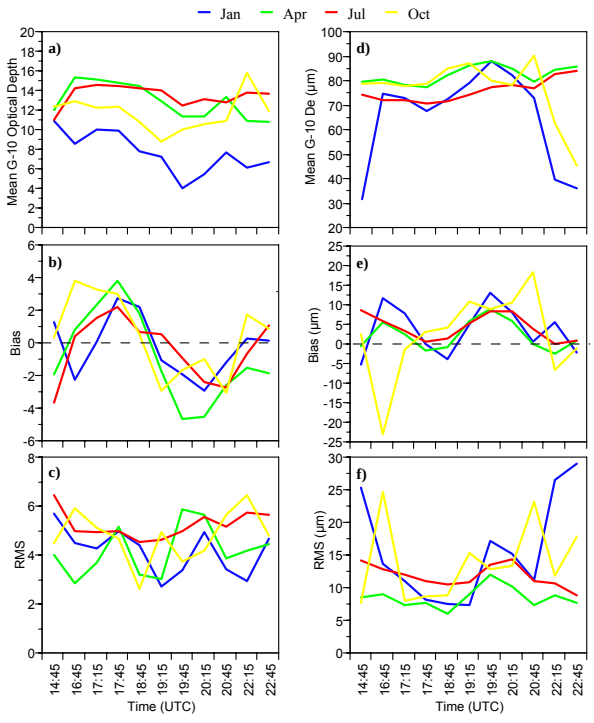

Figure 5. Summary of VISST derived G-10 hourly mean ice cloud τ and De with associated biases and RMS errors from comparison to G-12 retrievals for the 4 months studied.

Discussion

Although the optical depths shown are limited to 32, the results are similar for optical depths up to 128. The calculated instantaneous RMS errors reflect spatial sampling errors, in addition to random errors from actual versus true model variations and 3D cloud structure. The hourly mean bias errors are the best measure of uncertainties due to angular effects, including those from model assumptions and 3D cloud structure.

The variation of the biases with UTC arise from the systematic changes in scattering angle as seen in Figure 6, which shows pairs of scattering angles at selected hours for each month. The angles observed after 1845 UTC almost mirror those before 1845 UTC. The angles at 1845 UTC are not exactly the same, perhaps, explaining why the retrievals are not unbiased at that time. The reversal of angles explains why the biases change systematically from morning to afternoon. The larger biases observed at 1645 and 2045 UTC during October are likely due to the extreme angle pairs that occur at those times. One of the angles (177°) is very close to the direct backscatter position while the other is close to 118°. The water droplet scattering phase functions are very sensitive to the assumed droplet size distribution at certain angles, especially near the direct backscatter (Arduini et al. 2005). Additionally, the cloud sides will be most illuminated at the large scattering angle, enhancing 3D effects. The ice crystal phase function is extremely sensitive to particle shape around 177°, so any deviation from the assumed shape (hexagonal columns) is likely to cause extreme errors in the retrieval at the backscatter angles (Chepfer et al. 2002).

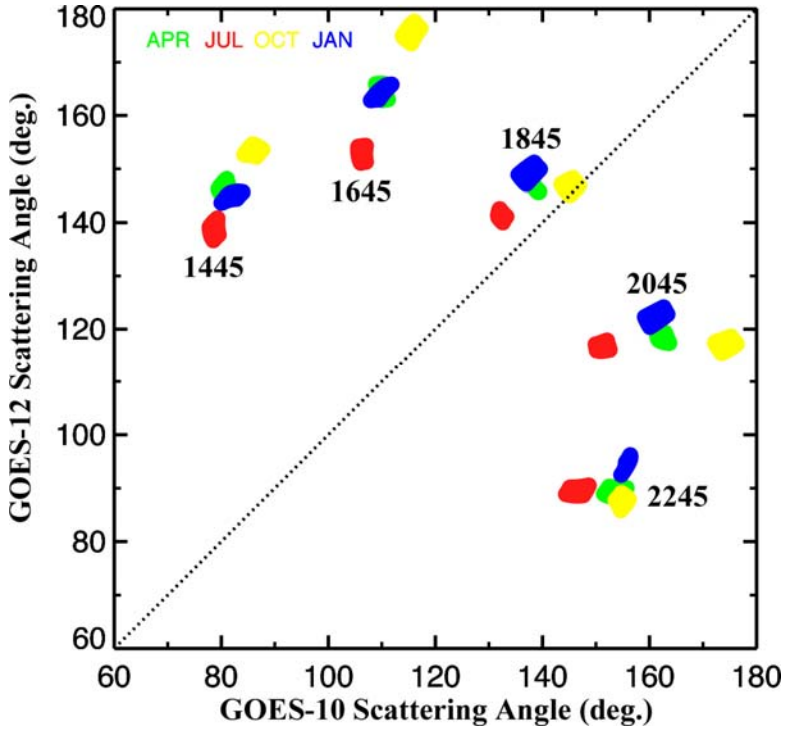

Figure 6. Hourly progression of matched scattering angle, color-coded by month of occurrence.

The extreme RMS values seen at the near-terminator hours are likely due to 3D effects because the longer shadows and greater retro-reflectance produced at those times are more likely to cause greater deviations from the plane-parallel theory used in the VISST parameterizations than at any other times. This is especially true for the ice clouds that have more potential for long shadows and cloud sides. Apparently, the increase in De that would be caused by shadows is more than balanced by the drop in De that should result from viewing the sunlit cloud sides when the sun is low (Figure 5d). The biases (Figure 5e) at those times are small because the scattering phase functions are similar for both views. Despite the differences in retrievals during forward and backscatter viewing conditions at particular times, these biases tend to be canceled out if averaged over the course of the day.

The water cloud errors are likely due to a variety of sources including 3D effects, the assumed droplet size distribution, and spatial mismatch because of differences in parallax and image time at the region of interest. The last item is most likely to affect the RMS differences while the 3D effects affect both. Preliminary results from Khaiyer et al. (2005) and Arduini et al. (2005) indicate that a broader size distribution could reduce the overall bias errors in LWP and Re substantially at each hour.

The observed errors in ice cloud optical depth retrievals are nearly twice as large as those from water clouds. Potentially, the use of other ice crystal models may lead to improved results from ice clouds as suggested by the dramatic errors at 1645 and 2045 UTC during October. Retrievals from ice clouds are subject to more errors than water clouds due to the effects of multi-layered clouds. The observed radiances can produce mixed ice and water signals that vary with the viewing angle angle.

Conclusions

VISST cloud properties derived from GOES data can be biased by angular effects. Differences between two satellite views can be as large as 15% for water clouds and as large as 20% for ice clouds at certain sets of angles or times of day. The actual true bias relative to the real optical depth or particle size is likely to be smaller than the difference between the two satellites because they can be biased in different directions from the true value. Representation of the diurnal cycle of cloud properties from geostationary satellites can be affected by these biases. However, calculation of daily averaged cloud properties is generally good. Potentially the calculation of cloud properties may be improved through the use varying particle size distributions and improved ice crystal models. The comparison of cloud retrievals from G-10 and G-12 show agreement for both ice and water clouds, that is consistent with observations from surface-satellite comparisons (e.g., Dong et al. 2002). The errors in retrieval of water cloud properties are smaller, as expected, due to simpler particle shapes and cloud uniformity. The error in retrieval of ice cloud properties was larger, as expected, due to more complex particle shapes and variation from cloud to cloud. Retrieval of thin cirrus cloud properties, which is highly dependent on accurate characterization of the scene background, could also be a major source of error.

Future Work

The analysis domain will be extended to provide additional scattering angle pairs to more adequately quantify angular biases. It will be expanded to include night time observations and algorithms. New water droplet distribution models will be implemented and tested to evaluate their effect on cloud

retrievals. New ice crystal phase functions will be implemented and tested to determine optimal values. The cloud retrievals will be evaluated to determine seasonal and diurnal cloud property variation. The optimal water and ice crystal models will be implemented. Three dimensional effects will be isolated by restricting samples by homogeneity of the scenes. Finally, validation studies using in-situ measurements from the Clouds and Radiation Testbed site and other regions will be used to verify the cloud retrievals in an independent manner.

Acknowledgements

The GOES data were obtained from the Space Science and Engineering Center at University of Wisconsin-Madison. This research was sponsored by ITF No. 214216-A-Q1 from Pacific Northwest National Laboratory.

References

Arduini, RF, P Minnis, WL Smith, Jr., JK Ayers, MM Khaiyer, and PW Heck. 2005. "Sensitivity of Satellite-Retrieved Cloud Properties to the Effective Variance of Cloud Droplet Size Distribution." In *Proceedings of the Fifteenth Annual ARM Science Team Meeting*, Daytona Beach, Florida, March 14 - 18.

Chepfer, H, P Minnis, DF Young, L Nguyen, and RF Arduini. 2002. "Estimation of cirrus cloud effective ice crystal shapes using visible reflectances from dual-satellite measurements." *Journal of Geophysical Research* 107 (D23), 10.1029/2000JD000240.

Dong, X, P Minnis, GG Mace, WL Smith, Jr., M Poellot, RT Marchand, and AD Rapp. 2002. Comparison of stratus cloud properties deduced from surface, GOES, and aircraft data during the March 2000 ARM Cloud IOP. *Journal of Atmospheric Science* 59, 3256-3284.

Khaiyer, MM, P Minnis, RF Arduini, PW Heck, R Palikonda, JK Ayers, DN Phan, and WL Smith, Jr. 2005. "Comparison of Cloud Liquid Water Paths over ARM SGP Using Satellite and Surface Data: Validation of New Models." In *Proceedings of the Fifteenth Annual ARM Science Team Meeting*, Daytona Beach, Florida, March 14 – 18.

Minnis, P, WL Smith, Jr., DF Young, L Nguyen, AD Rapp, PW Heck, S. Sun-Mack, QZ Trepte, and Y Chen. 2001. "A near-real time method for deriving cloud and radiation properties from satellites for weather and climate studies." In *Proceedings of the AMS Eleventh Conference Satellite Meteorology and Oceanography*, Madison, Wisconsin, October 15-18, p. 4-19.

Minnis, P, DP Garber, DF Young, RF Arduini, and Y Takano. 1998. "Parameterization of reflectance and effective emittance for satellite remote sensing of cloud properties." *Journal of Atmospheric Science* 55, 3313-3339.

Minnis, P, L Nguyen, WL Smith, Jr., MM Khaiyer, R Palikonda, DA Spangenberg, DR Doelling, D Phan, GD Nowicki, PW Heck, and C Wolff. 2004. "Real-time cloud, radiation, and aircraft icing parameters from GOES over the USA." In *Proceedings of the Thirteenth AMS Conference Satellite Oceanography and Meteorology*, Norfolk, Virginia, September 20-24, CD-ROM, P7.1.

Trepte, Q, Y Chen, S Sun-Mack, P Minnis, DF Young, BA Baum, and PW Heck. 1999. "Scene identification for the CERES cloud analysis subsystem." In *Proceedings of the AMS Tenth Conference Atmospheric Radiation*, Madison, Wisconsin, June 28 – July 2, 169-172.